



WORK VIII 2025 Eta

WORKSHOP EM MODELAGEM NUMÉRICA DE TEMPO, CLIMA
E MUDANÇAS CLIMÁTICAS UTILIZANDO O MODELO ETA

Planetary Boundary Layer Parameterization for High-Resolution Mesoscale Simulations

Branko Kosović,
Johns Hopkins University

Ralph O'Connor Sustainable Energy Institute

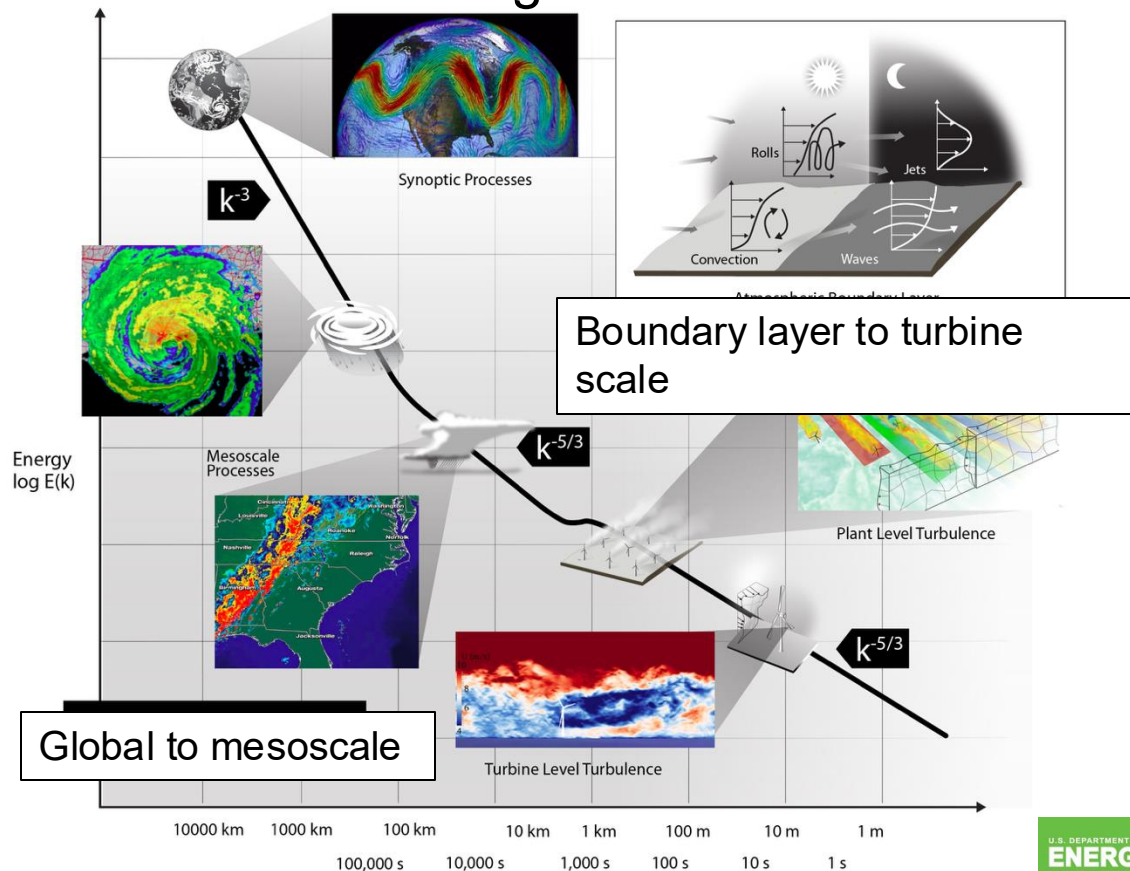
August 26, 2025

Many colleagues contributed to the multiscale modeling research



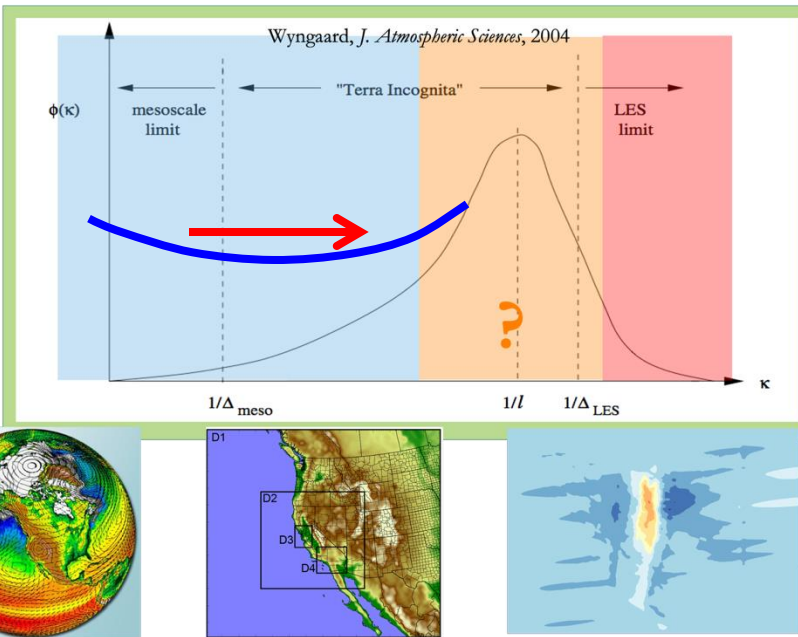
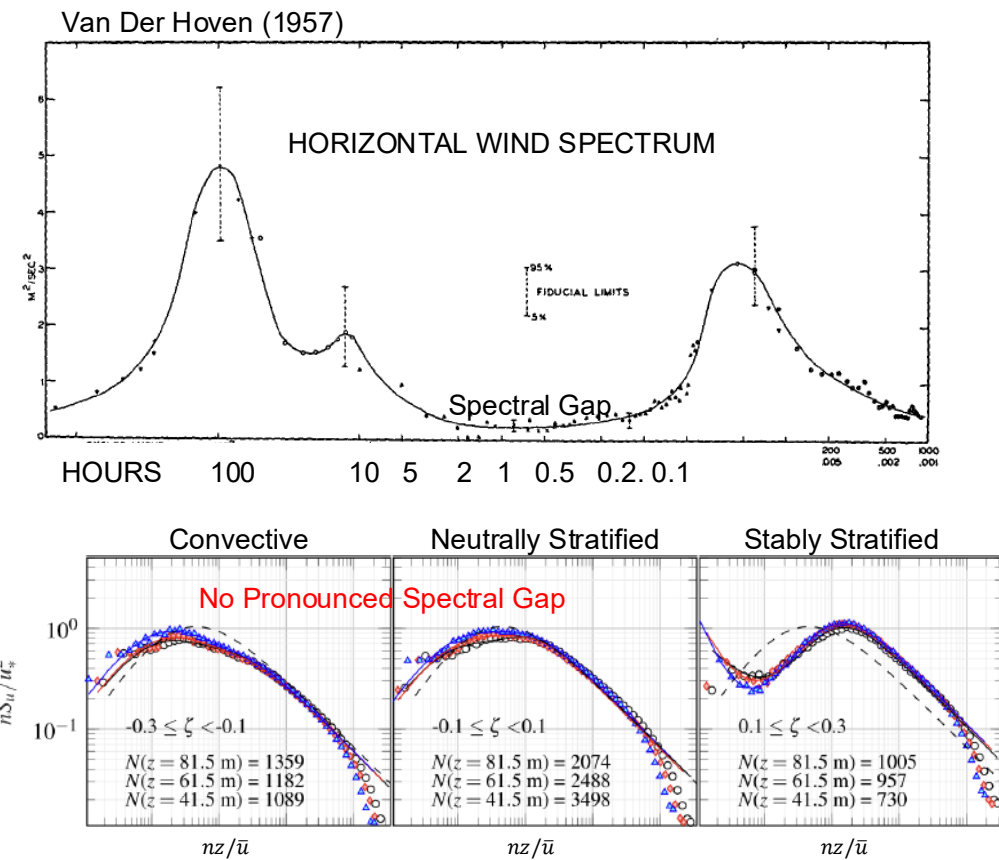
Domingo Muñoz-Esparza, Pedro Jiménez, Timothy W. Juliano, Sue Ellen Haupt
Jeremy Sauer, Masih Eghdami, Eric Hendricks

For many applications, atmospheric boundary layer cannot be isolated from the larger scale flows



- Various applications including wind energy require high-resolution observations and simulations,
- However, for many applications, the ABL cannot be studied in isolation from larger scale atmospheric motions.
- Nesting LES domains within a mesoscale domain enables resolving large turbulent eddies.
- NWP models, including the Weather Research and Forecasting (WRF) model, now enable such nesting.

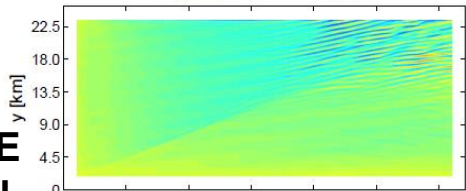
CHALLENGE: What is the effective approach to simulating mesoscale-microscale interactions?



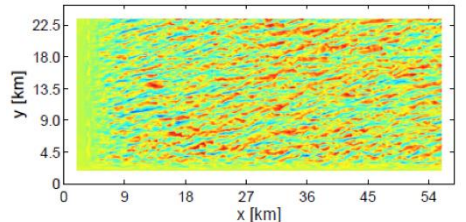
Adapted from Mirocha (LLNL)

CODES (NESTING vs. GRID REFINEMENT)

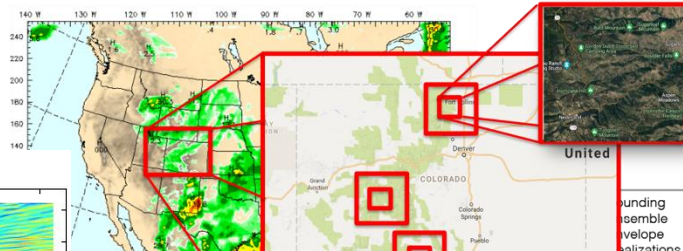
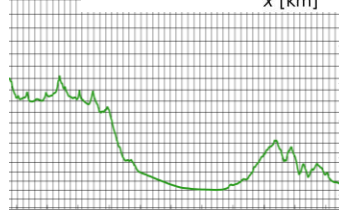
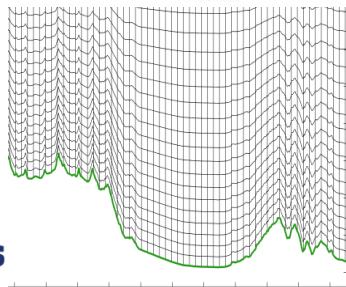
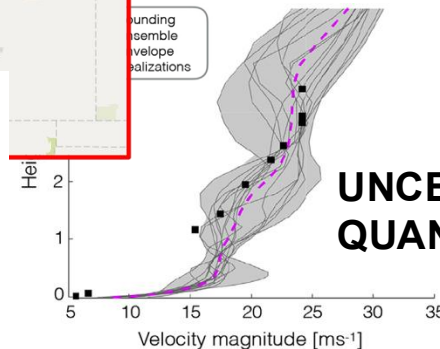
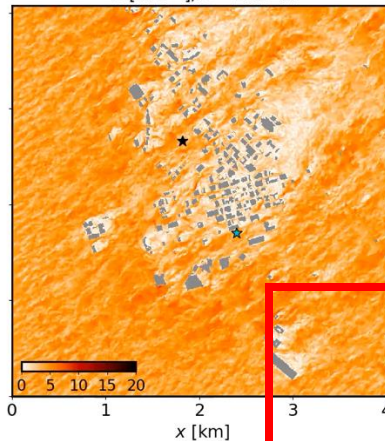
NBA TKE, u at z=100 m



CELL PERTURBATION



GRIDS & BUNDARY CONDITIONS

Energy at **Hopkins** $U \text{ [m s}^{-1}\text{]}, z = 26.5 \text{ m}$ 

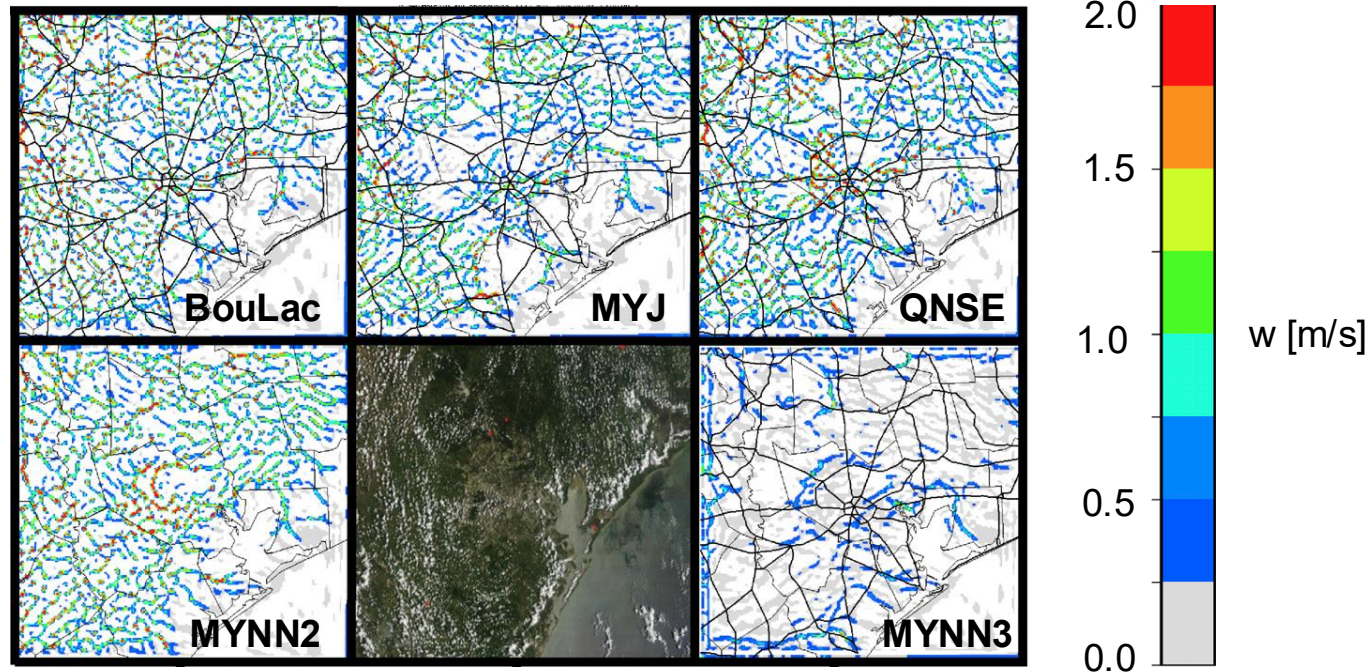
UNCERTAINTY QUANTIFICATION

[illegible]

PARAMETERIZATIONS

Simulations of daytime ABL in Houston – Galveston area using various PBL schemes result in different convectively induced secondary circulations (CISC)

$\Delta x = 1 \text{ km}$



Ching et al. (2014, MWR) comment: “However, with limited resolution, energy exchanges between CISCs and smaller-scale turbulence are not represented and hence a distorted picture of the CISCs can emerge.” (see also Zhou et al. 2014, JAS)

USGS

Capacity (MW)

0 1 2 3 4

AUC HOO SML BID GDH ROO

AO8 AO7 The Dalles AO5 WAS AO6 AO4 AO2

~70 km

Mount Hood

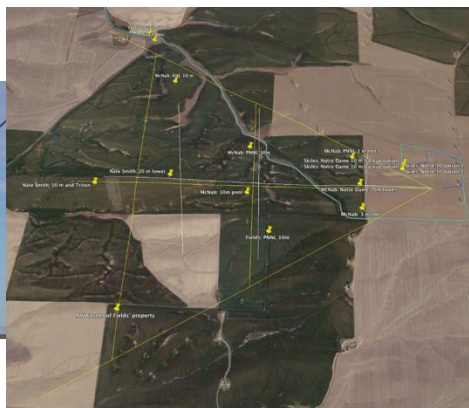
red arrows – met towers
yellow squares – sodars
green circles – turbines

D03 – 60x30km

10 m

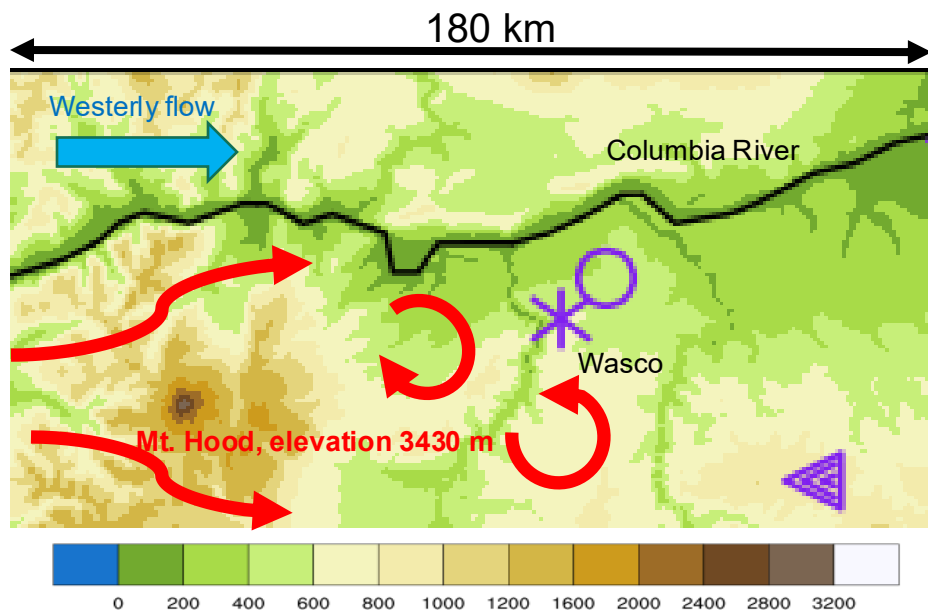


Energy at **Hopkins**



ABL structure observed and simulated in the WFIP2 project is significantly affected by complex terrain upwind

LES domains over the WFIP2 field study area
WRF – Domain 2 – grid-cell size 30 m
6000 x 3000 grid cells

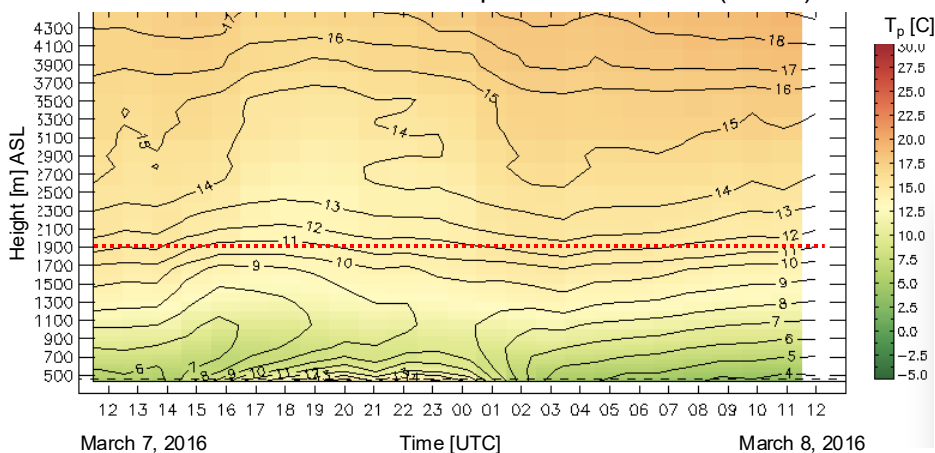


Energy at Hopkins

Potential temperature at Wasco March 7, 2015

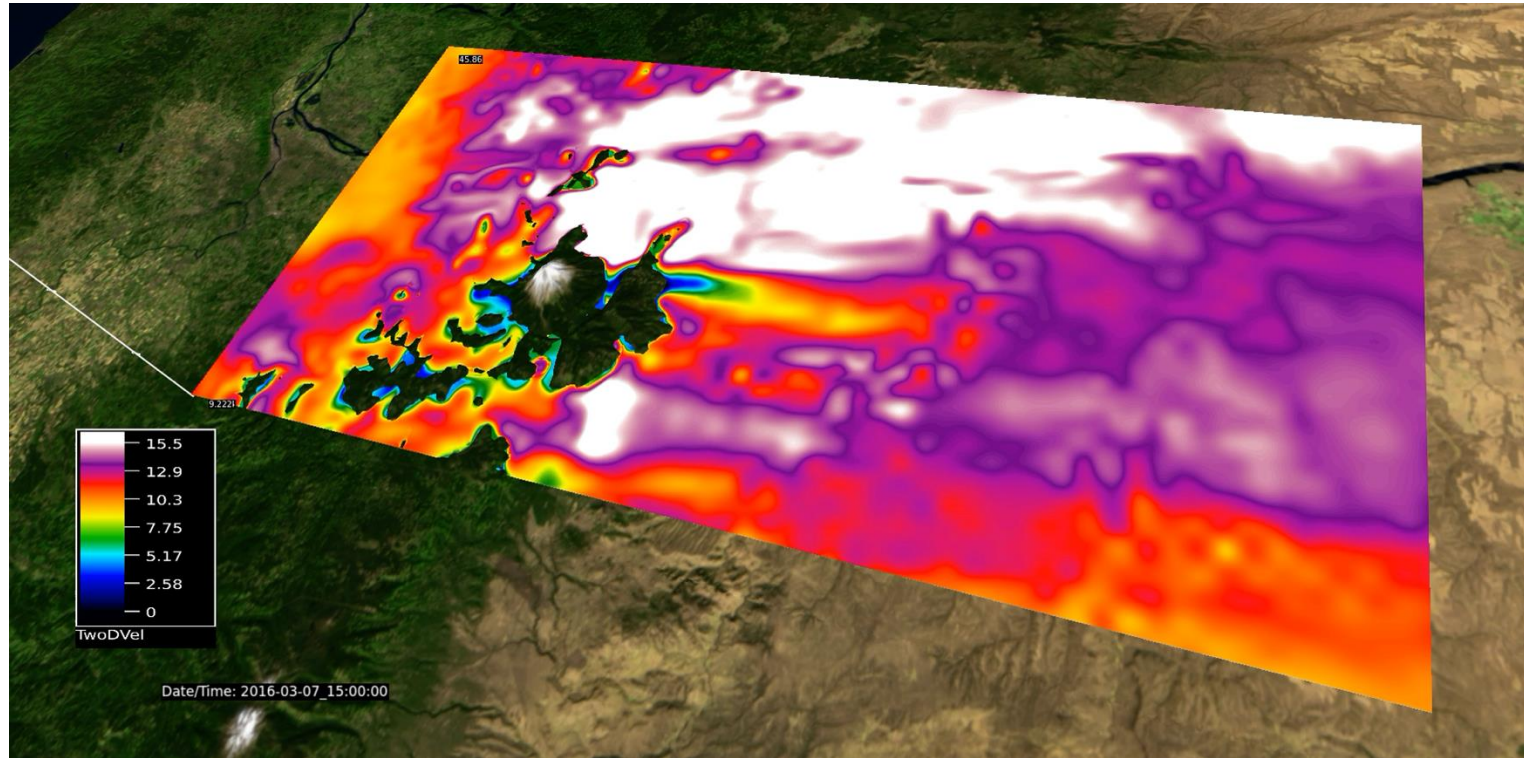
Inversion was at about 1900 m ASL – below the top of Mt. Hood. Westerly flow splits around Mt. Hood, potentially leading to shedding of von Kármán vortices.

NOAA/ESRL Observed Potential Temperature at Wasco (458 m)



High-resolution, large-eddy simulations are used to improve numerical weather prediction models

Horizontal velocity at 1200 m above mean sea level



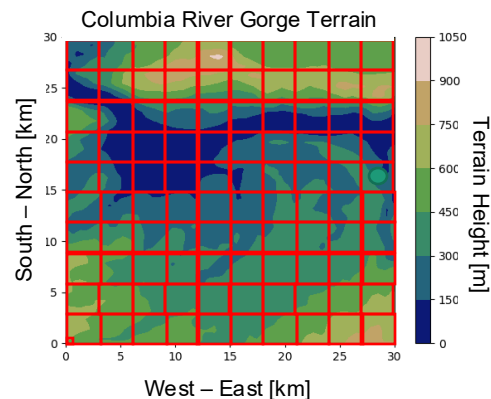
We used LES of Mt Hood flow to assess the relative importance of horizontal shear and horizontal turbulent stress divergence

Ratio of horizontal to vertical shear magnitude

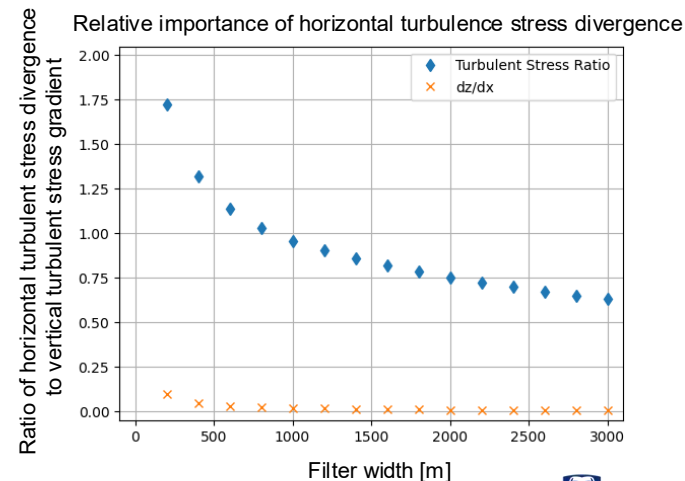
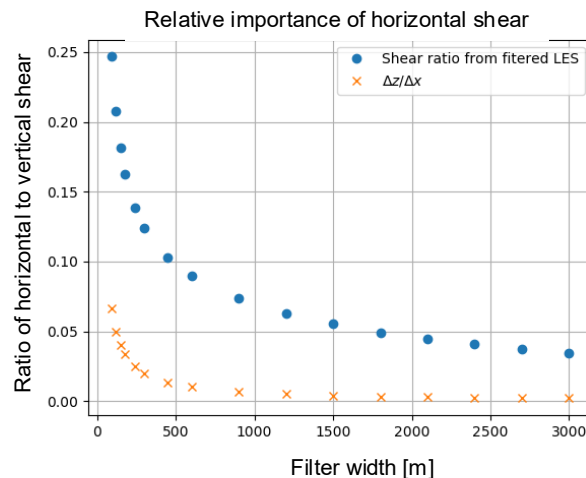
$$R_S = \left[\frac{\left(\frac{\partial u}{\partial x}\right)^2 + \left(\frac{\partial u}{\partial y}\right)^2 + \left(\frac{\partial v}{\partial x}\right)^2 + \left(\frac{\partial v}{\partial y}\right)^2}{\left(\frac{\partial u}{\partial z}\right)^2 + \left(\frac{\partial v}{\partial z}\right)^2} \right]^{\frac{1}{2}}$$

Ratio of horizontal turbulent stress divergence to vertical turbulent stress gradient

$$R_{TS} = \left[\frac{\left(\frac{\partial \overline{uu}}{\partial x}\right)^2 + \left(\frac{\partial \overline{uv}}{\partial x}\right)^2 + \left(\frac{\partial \overline{uv}}{\partial y}\right)^2 + \left(\frac{\partial \overline{vv}}{\partial y}\right)^2}{\left(\frac{\partial \overline{uw}}{\partial z}\right)^2 + \left(\frac{\partial \overline{vw}}{\partial z}\right)^2} \right]^{\frac{1}{2}}$$



We filtered LES of the flow east of Mt Hood at different scales and computed two ratios.



In NWP models, the assumption is that turbulence is horizontally homogeneous over a grid cell and it is parameterized using 1D schemes

Conservation equation for the horizontal wind components:

$$\begin{aligned}\frac{\partial U}{\partial t} + U_j \frac{\partial U}{\partial x_j} &= \frac{1}{\rho} \frac{\partial P}{\partial x} - fV - \frac{\partial \overline{uw}}{\partial z} \\ \frac{\partial V}{\partial t} + U_j \frac{\partial V}{\partial x_j} &= \frac{1}{\rho} \frac{\partial P}{\partial y} + fU - \frac{\partial \overline{vw}}{\partial z}\end{aligned}$$

- 1D PBL closure is based on assumption of homogeneity over a grid cell
- Vertical turbulent fluxes are parameterized by the PBL scheme (e.g., MYNN, YSU, etc.)
- Horizontal diffusion is “parameterized” using 2D Smagorinsky type model (Smagorinsky 1963)
- 2D Smagorinsky model is introduced for numerical stability (Smagorinsky 1990)

To account for the effects of horizontal shear and horizontal component of stress divergence, we implemented a 3D PBL scheme

- 3D PBL scheme includes diagnostic parameterization of all six turbulent stress components, three turbulent sensible heat flux components, and three moisture flux components
- Full 3D turbulent stress and flux divergence is computed

$$\frac{\partial U_i}{\partial t} + U_j \frac{\partial U_i}{\partial x_j} = -\frac{1}{\rho} \frac{\partial P}{\partial x_i} + 2\epsilon_{ijk}\Omega_j U_k - \frac{\partial \langle u_i u_j \rangle}{\partial x_j}$$

- The implementation is based on Mellor and Yamada (1982) level 2½ model including a prognostic equation for TKE
- Objective was to implement a consistent formulation for all turbulent fluxes base on the Reynolds Averaged Navier-Stokes equations (Kosović et al., 2020, *J Phys. Conf. Ser.*; Juliano et al., 2021, *MWR*; Eghdami et al., 2022, *MWR*)

The need for 3D PBL scheme is supported by the analysis of relative importance of horizontal shear terms

$$\begin{bmatrix}
 \frac{q}{2\ell_1} + 2\frac{\partial U}{\partial x} & -\frac{\partial V}{\partial y} & -\frac{\partial W}{\partial z} & 2\frac{\partial U}{\partial y} - \frac{\partial V}{\partial x} & 2\frac{\partial U}{\partial z} - \frac{\partial W}{\partial x} & -\frac{\partial V}{\partial z} - \frac{\partial W}{\partial y} & 0 & 0 & \beta g & 0 \\
 -\frac{\partial U}{\partial x} & \frac{q}{2\ell_1} + 2\frac{\partial V}{\partial y} & -\frac{\partial W}{\partial z} & 2\frac{\partial V}{\partial x} - \frac{\partial U}{\partial y} & -\frac{\partial U}{\partial z} - \frac{\partial W}{\partial x} & 2\frac{\partial V}{\partial z} - \frac{\partial W}{\partial y} & 0 & 0 & \beta g & 0 \\
 -\frac{\partial U}{\partial x} & -\frac{\partial V}{\partial y} & \frac{q}{2\ell_1} + 2\frac{\partial W}{\partial z} & -\frac{\partial U}{\partial y} - \frac{\partial V}{\partial x} & 2\frac{\partial W}{\partial x} - \frac{\partial U}{\partial z} & 2\frac{\partial W}{\partial x} - \frac{\partial V}{\partial z} & 0 & 0 & -2\beta g & 0 \\
 \frac{\partial V}{\partial x} & \frac{\partial U}{\partial y} & 0 & \frac{q}{3\ell_1} + \frac{\partial U}{\partial x} + \frac{\partial V}{\partial y} & \frac{\partial V}{\partial z} & \frac{\partial U}{\partial z} & 0 & 0 & 0 & 0 \\
 \frac{\partial W}{\partial x} & 0 & \frac{\partial U}{\partial z} & \frac{\partial W}{\partial y} & \frac{q}{3\ell_1} + \frac{\partial U}{\partial x} + \frac{\partial W}{\partial z} & \frac{\partial U}{\partial y} & -\beta g & 0 & 0 & 0 \\
 0 & \frac{\partial W}{\partial y} & \frac{\partial V}{\partial z} & \frac{\partial W}{\partial x} & \frac{\partial V}{\partial x} & \frac{q}{3\ell_1} + \frac{\partial V}{\partial y} + \frac{\partial W}{\partial z} & 0 & -\beta g & 0 & 0 \\
 \frac{\partial \theta}{\partial x} & 0 & 0 & \frac{\partial \theta}{\partial y} & \frac{\partial \theta}{\partial z} & 0 & \frac{q}{3\ell_2} + \frac{\partial U}{\partial x} & \frac{\partial U}{\partial y} & \frac{\partial U}{\partial z} & 0 \\
 0 & \frac{\partial \theta}{\partial y} & 0 & \frac{\partial \theta}{\partial x} & 0 & \frac{\partial \theta}{\partial z} & \frac{\partial V}{\partial x} & \frac{q}{3\ell_2} + \frac{\partial V}{\partial y} & \frac{\partial V}{\partial z} & 0 \\
 0 & 0 & \frac{\partial \theta}{\partial z} & 0 & \frac{\partial \theta}{\partial x} & \frac{\partial \theta}{\partial y} & \frac{\partial W}{\partial x} & \frac{\partial W}{\partial y} & \frac{q}{3\ell_2} + \frac{\partial W}{\partial z} & -\beta g \\
 0 & 0 & 0 & 0 & 0 & 0 & \frac{\partial \theta}{\partial x} & \frac{\partial \theta}{\partial y} & \frac{\partial \theta}{\partial z} & \frac{q}{\Lambda_2}
 \end{bmatrix}
 \begin{bmatrix}
 \overline{u^2} \\
 \overline{v^2} \\
 \overline{w^2} \\
 \overline{uv} \\
 \overline{uw} \\
 \overline{vw} \\
 \overline{u\theta} \\
 \overline{v\theta} \\
 \overline{w\theta} \\
 \overline{\theta^2}
 \end{bmatrix}$$

The need for 3D PBL scheme is supported by the analysis of relative importance of horizontal shear terms

$\frac{q}{2\ell_1} + 2\frac{\partial U}{\partial x}$	$-\frac{\partial V}{\partial y}$	$-\frac{\partial W}{\partial z}$	$2\frac{\partial U}{\partial y} - \frac{\partial V}{\partial x}$	$2\frac{\partial U}{\partial z} - \frac{\partial W}{\partial x}$	$-\frac{\partial V}{\partial z} - \frac{\partial W}{\partial y}$	0	0	βg	0	$\overline{u^2}$
$-\frac{\partial U}{\partial x}$	$\frac{q}{2\ell_1} + 2\frac{\partial V}{\partial y}$	$-\frac{\partial W}{\partial z}$	$2\frac{\partial V}{\partial x} - \frac{\partial U}{\partial y}$	$-\frac{\partial U}{\partial z} - \frac{\partial W}{\partial x}$	$2\frac{\partial V}{\partial z} - \frac{\partial W}{\partial y}$	0	0	βg	0	$\overline{v^2}$
$-\frac{\partial U}{\partial x}$	$-\frac{\partial V}{\partial y}$	$\frac{q}{2\ell_1} + 2\frac{\partial W}{\partial z}$	$-\frac{\partial U}{\partial y} - \frac{\partial V}{\partial x}$	$2\frac{\partial W}{\partial x} - \frac{\partial U}{\partial z}$	$2\frac{\partial W}{\partial x} - \frac{\partial V}{\partial z}$	0	0	$-2\beta g$	0	$\overline{w^2}$
$\frac{\partial V}{\partial x}$	$\frac{\partial U}{\partial y}$	0	$\frac{q}{3\ell_1} + \frac{\partial U}{\partial x} + \frac{\partial V}{\partial y}$	$\frac{\partial V}{\partial z}$	$\frac{\partial U}{\partial z}$	0	0	0	0	\overline{uw}
$\frac{\partial W}{\partial x}$	0	$\frac{\partial U}{\partial z}$	$\frac{\partial W}{\partial y}$	$\frac{q}{3\ell_1} + \frac{\partial U}{\partial x} + \frac{\partial W}{\partial z}$	$\frac{\partial U}{\partial y}$	$-\beta g$	0	0	0	\overline{vw}
0	$\frac{\partial W}{\partial y}$	$\frac{\partial V}{\partial z}$	$\frac{\partial W}{\partial x}$	$\frac{\partial V}{\partial x}$	$\frac{q}{3\ell_1} + \frac{\partial V}{\partial y} + \frac{\partial W}{\partial z}$	0	$-\beta g$	0	0	
$\frac{\partial \theta}{\partial x}$	0	0	$\frac{\partial \theta}{\partial y}$	$\frac{\partial \theta}{\partial z}$	0	$\frac{q}{3\ell_2} + \frac{\partial U}{\partial x}$	$\frac{\partial U}{\partial y}$	$\frac{\partial U}{\partial z}$	0	$\overline{u\theta}$
0	$\frac{\partial \theta}{\partial y}$	0	$\frac{\partial \theta}{\partial x}$	0	$\frac{\partial \theta}{\partial z}$	$\frac{\partial V}{\partial x}$	$\frac{q}{3\ell_2} + \frac{\partial V}{\partial y}$	$\frac{\partial V}{\partial z}$	0	$\overline{v\theta}$
0	0	$\frac{\partial \theta}{\partial z}$	0	$\frac{\partial \theta}{\partial x}$	$\frac{\partial \theta}{\partial y}$	$\frac{\partial W}{\partial x}$	$\frac{\partial W}{\partial y}$	$\frac{q}{3\ell_2} + \frac{\partial W}{\partial z}$	$-\beta g$	$\overline{w\theta}$
0	0	0	0	0	0	$\frac{\partial \theta}{\partial x}$	$\frac{\partial \theta}{\partial y}$	$\frac{\partial \theta}{\partial z}$	$\frac{q}{\Lambda_2}$	$\overline{\theta^2}$

Notice that horizontal shear terms are also multiplying dominant turbulent stress terms (in orange rectangles).

Using PBL approximation and neglecting horizontal derivatives, we can obtain a simplified system of equations

$$\begin{bmatrix}
 \frac{q}{2\ell_1} & 0 & 0 & 0 & 2\frac{\partial U}{\partial z} & -\frac{\partial V}{\partial z} & 0 & 0 & \beta g & 0 \\
 0 & \frac{q}{2\ell_1} & 0 & 0 & -\frac{\partial U}{\partial z} & 2\frac{\partial V}{\partial z} & 0 & 0 & \beta g & 0 \\
 0 & 0 & \frac{q}{2\ell_1} & 0 & -\frac{\partial U}{\partial z} & -\frac{\partial V}{\partial z} & 0 & 0 & -2\beta g & 0 \\
 0 & 0 & 0 & \frac{q}{3\ell_1} & \frac{\partial V}{\partial z} & \frac{\partial U}{\partial z} & 0 & 0 & 0 & 0 \\
 0 & 0 & \frac{\partial U}{\partial z} & 0 & \frac{q}{3\ell_1} & 0 & -\beta g & 0 & 0 & 0 \\
 0 & 0 & \frac{\partial V}{\partial z} & 0 & 0 & \frac{q}{3\ell_1} & 0 & -\beta g & 0 & 0 \\
 0 & 0 & 0 & 0 & \frac{\partial \Theta}{\partial z} & 0 & \frac{q}{3\ell_2} & 0 & \frac{\partial U}{\partial z} & 0 \\
 0 & 0 & 0 & 0 & 0 & \frac{\partial \Theta}{\partial z} & 0 & \frac{q}{3\ell_2} & \frac{\partial V}{\partial z} & 0 \\
 0 & 0 & \frac{\partial \Theta}{\partial z} & 0 & 0 & 0 & 0 & 0 & \frac{q}{3\ell_2} & -\beta g \\
 0 & 0 & 0 & 0 & 0 & 0 & 0 & 0 & \frac{\partial \Theta}{\partial z} & \frac{q}{\Lambda_2}
 \end{bmatrix}
 \begin{bmatrix}
 \overline{u^2} \\
 \overline{v^2} \\
 \overline{w^2} \\
 \overline{uv} \\
 \overline{uw} \\
 \overline{vw} \\
 \overline{u\theta} \\
 \overline{v\theta} \\
 \overline{w\theta} \\
 \overline{\theta^2}
 \end{bmatrix}
 =
 \begin{bmatrix}
 \frac{q^3}{6\ell_1} \\
 \frac{q^3}{6\ell_1} \\
 \frac{q^3}{6\ell_1} \\
 0 \\
 C_1 q^2 \frac{\partial U}{\partial z} \\
 C_1 q^2 \frac{\partial V}{\partial z} \\
 0 \\
 0 \\
 0 \\
 0
 \end{bmatrix}$$

In addition to the set of algebraic equations for turbulent stresses and fluxes, we also solve a prognostic equation for TKE

$$\frac{q^3}{\Lambda_1} = -\overline{u^2} \frac{\partial U}{\partial x} - \overline{v^2} \frac{\partial V}{\partial y} - \overline{w^2} \frac{\partial W}{\partial z} - \overline{uv} \left(\frac{\partial U}{\partial y} + \frac{\partial V}{\partial x} \right) - \overline{uw} \left(\frac{\partial U}{\partial z} + \frac{\partial W}{\partial x} \right) - \overline{vw} \left(\frac{\partial V}{\partial z} + \frac{\partial W}{\partial y} \right) - \beta g \overline{w\theta}$$

Here, ℓ_1 , Λ_1 , ℓ_2 , and Λ_2 are length scales that are proportional to each other, so they can be expressed in terms of a master length scale ℓ :

$$[\ell_1 \quad \Lambda_1 \quad \ell_2 \quad \Lambda_2] = \ell [A_1 \quad B_1 \quad A_2 \quad B_2]$$

Master length scale is defined by Bougeault and Lacarrere (1989) as:

$$\int_z^{z+l_{up}} \beta[\theta(z) - \theta(z')] dz' = E(z) \quad \int_{z-l_{up}}^z \beta[\theta(z') - \theta(z)] dz' = E(z)$$

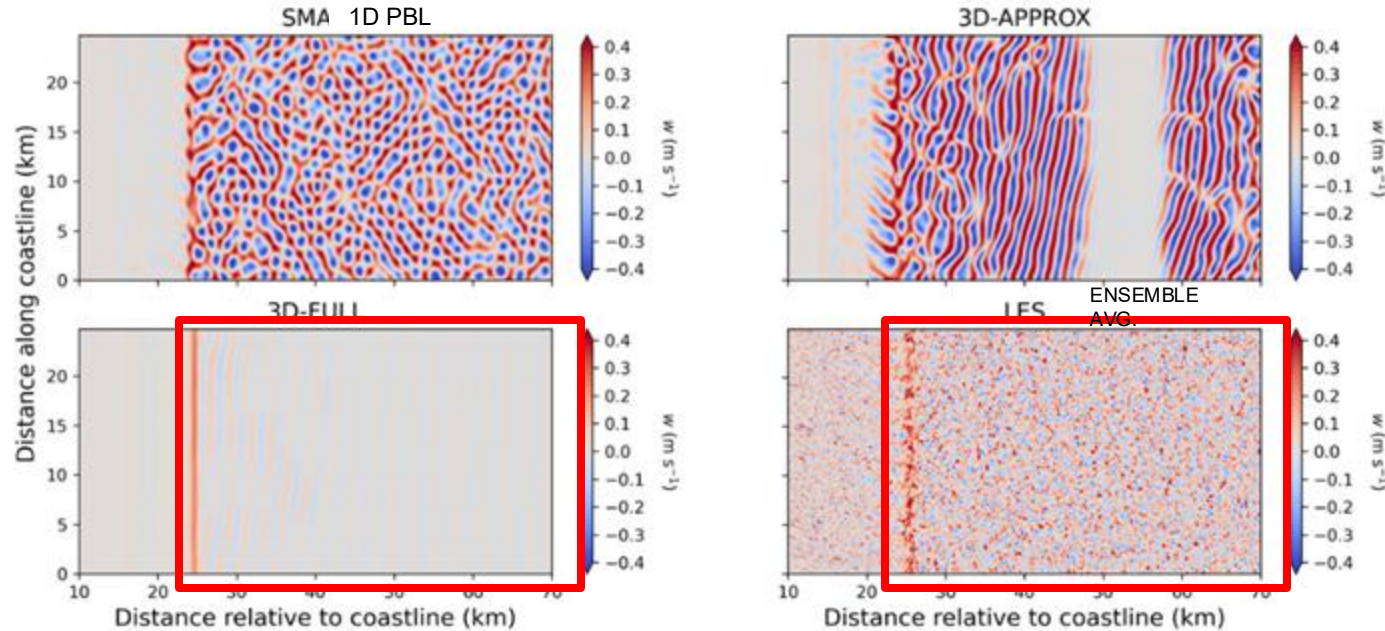
$$l_\epsilon = (l_{up} l_{down})^{1/2} ; l_k = \min(l_{up}, l_{down})$$

The constants, A_1 , B_1 , A_2 , B_2 , and C_1 were determined using LES:

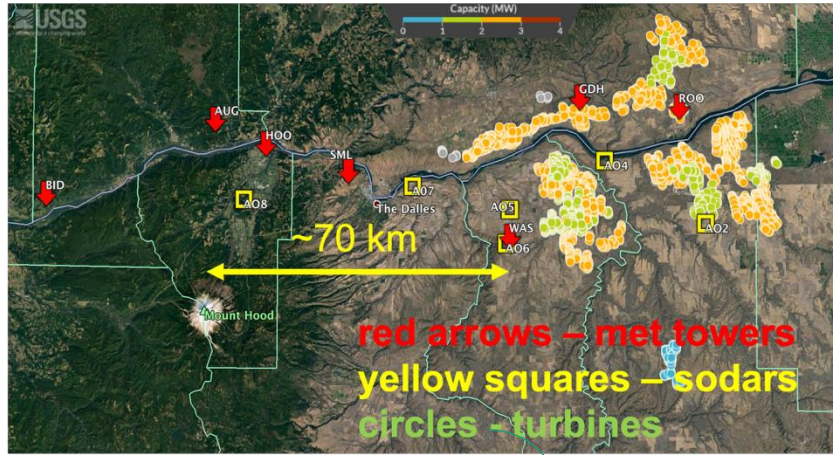
$$[A_1 \quad B_1 \quad A_2 \quad B_2 \quad C_1] = [0.3 \quad 8.4 \quad 0.33 \quad 6.4 \quad 0.08]$$

Full 3D PBL parameterization results in improved sea breeze simulations

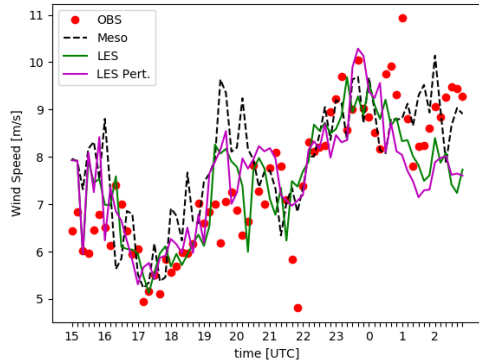
Sea breeze front initiation



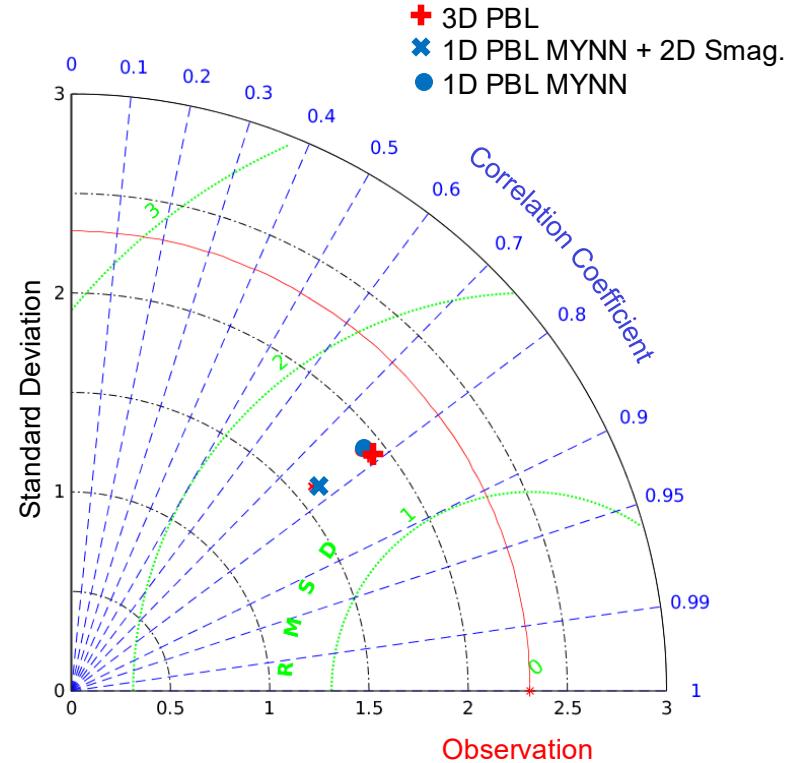
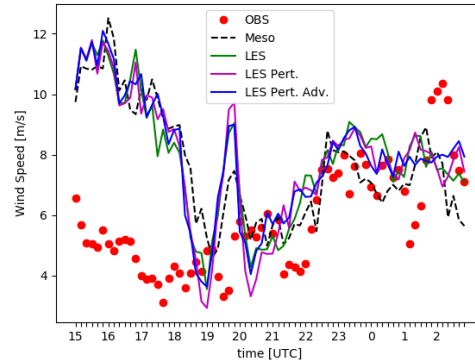
We have tested the 3D PBL scheme and LES using WFIP2 data



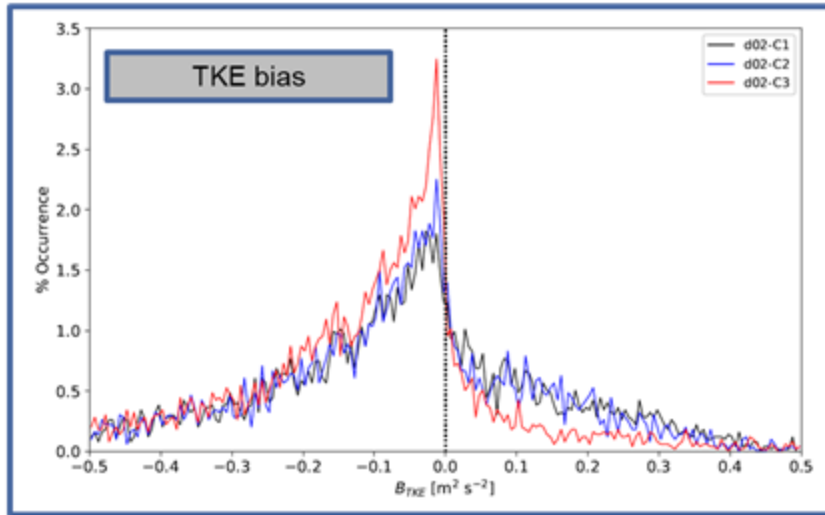
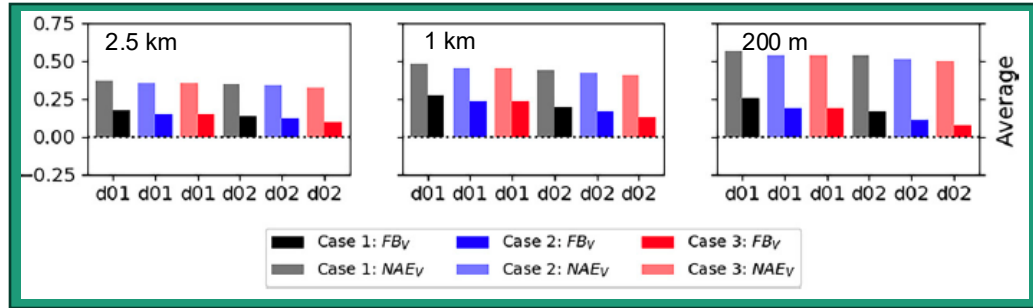
Sodar AON5



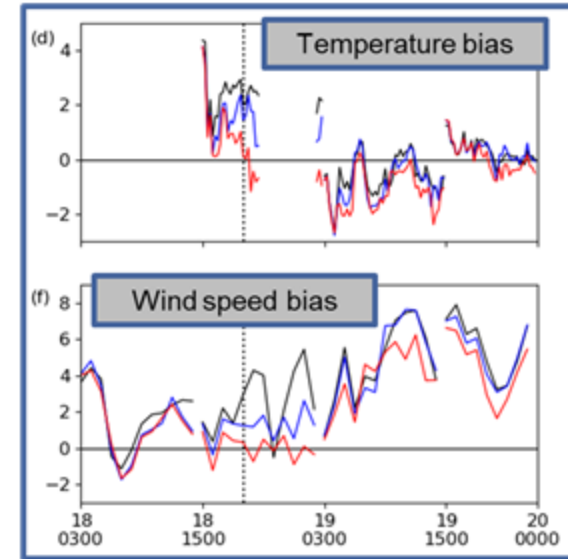
Sodar AON6



Modeling of cold pool erosion during WFIP2 improved using a version 3D PBL parameterization

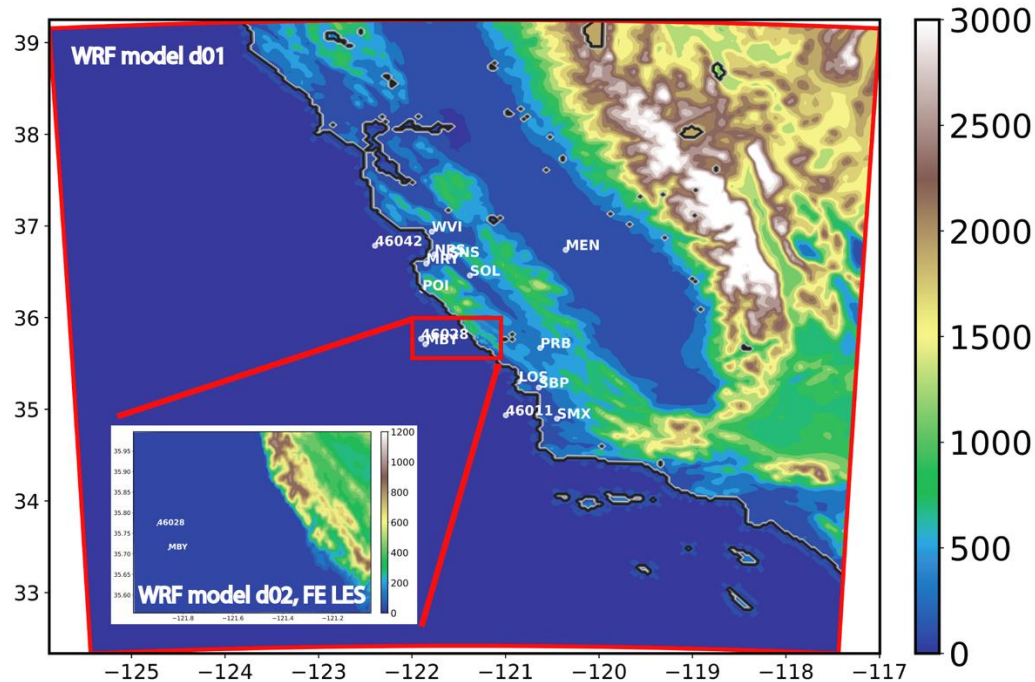


Case name	Turbulence Closure
Case 1	MYNN; along coordinate sfc
Case 2	MYNN; in physical space
Case 3	3D-APPROX; in physical space



Day/Time in January 2017 [UTC]

We simulated a strong coastal jet observed on May 8, 2021 along the coast of California and compared 3D PBL scheme to 1D scheme and upscaled LES

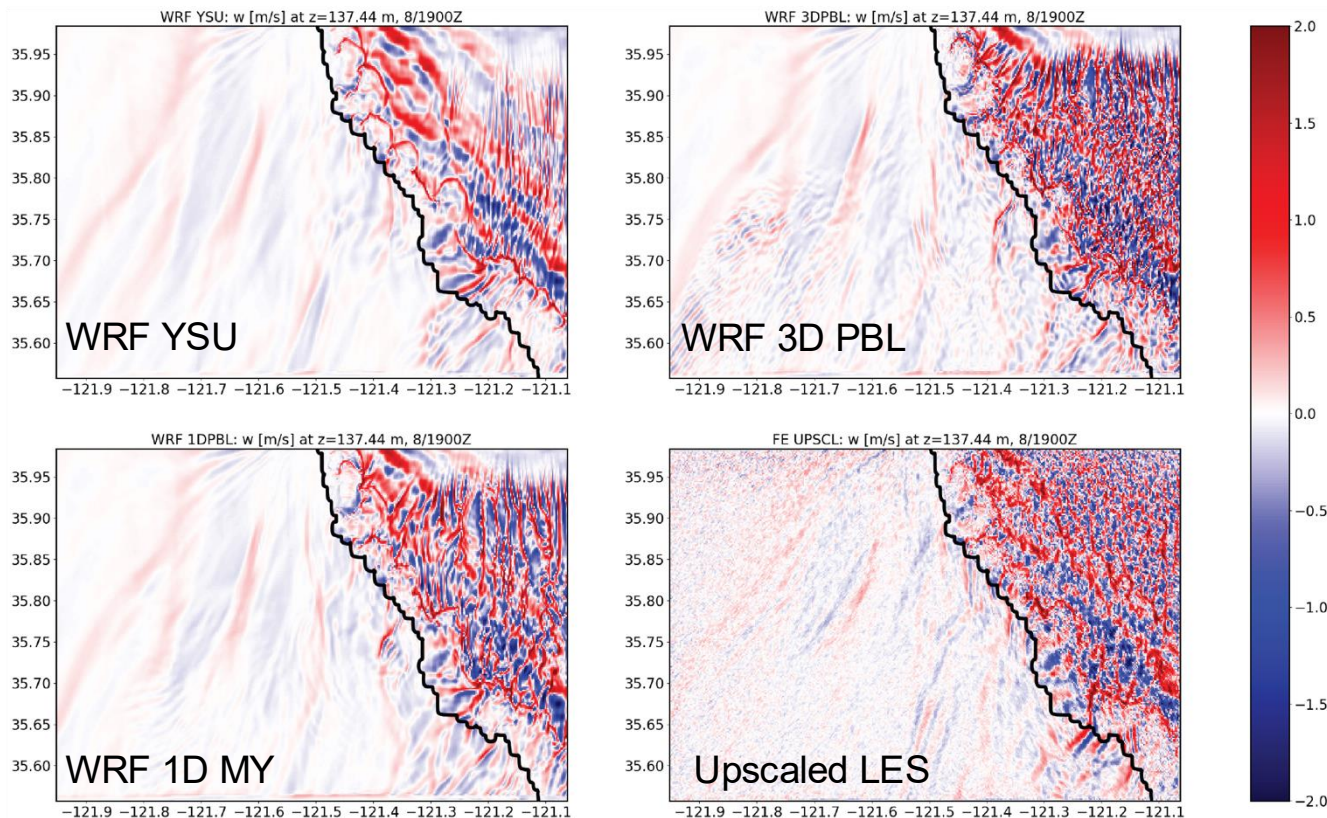


D01 – $\Delta x = 1$ km

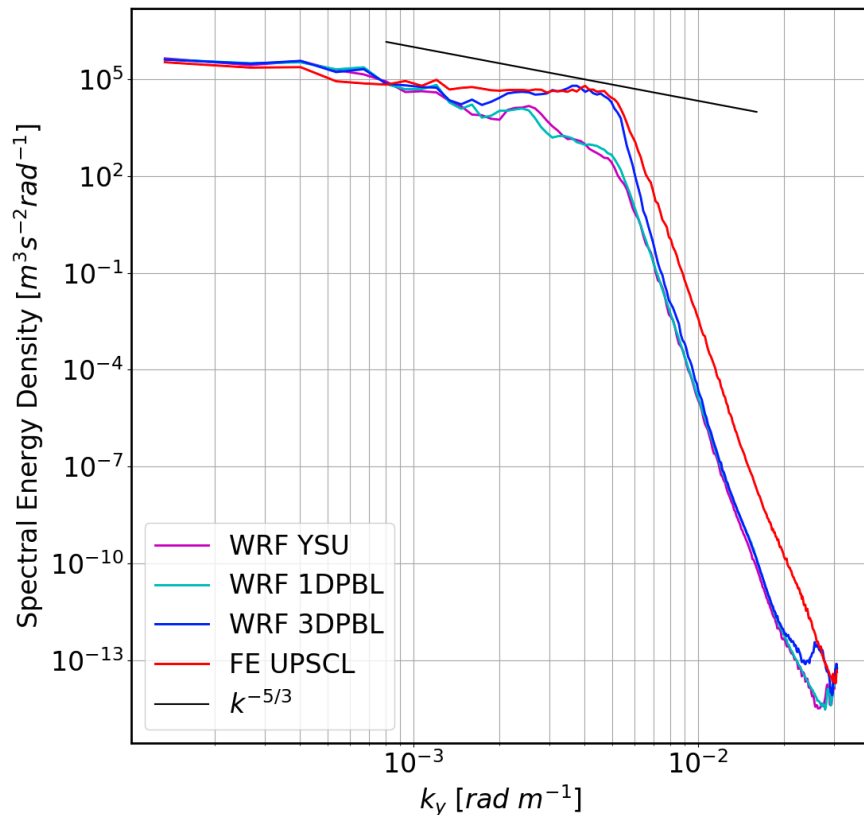
D02 – $\Delta x = 200$ m

Hendricks et al. (manuscript in preparation)

Convective structures produced by 3D PBL are more similar to those from upscaled LES than those produced by 1D PBLs, YSU and MY



Wind speed spectra computed over ocean from these simulations confirm observation that 3D PBL represents small scales better than 1D schemes



When modeling turbulent stresses and fluxes we need to define the averaging operator

Ensemble Average

Strictly - phase space average approximated by an average over a number of samples

$$\bar{\phi} = \frac{1}{N} \sum_{i=1}^N \phi_i$$



Volume Average

Introduces grid dependence, i.e., length scales vary with the grid size

$$\bar{\phi} = \frac{1}{V} \int_{\Omega} \phi \, dV$$

“In practice, the flow is neither stationary nor homogeneous, so that alternate averaging operators must be sought that are suitable for typical cloud and mesoscale fields. In the case of numerical weather prediction (NWP) models, it has become common to define an averaging operator that is related to the grid scale.”

Collins, W. R., 1986: Averaging and the Parameterization of Physical Processes in Mesoscale Models. In “Mesoscale Meteorology and Forecasting” ed. Peter S. Ray, AMS, Boston 1986.

Goal: Use LES with different stabilities and resolutions to estimate the length scales in the 3D PBL parameterization

Mellor Yamada Level 2 model:

$$\frac{\partial q^2}{\partial t} + U_k \frac{\partial q^2}{\partial x_k} = \frac{\partial}{\partial x_k} \left[\langle u_k (q^2 + p/\rho_0) \rangle \right] + 2 \left[(\langle u_i u_j \rangle \partial U_i / \partial x_j + \beta g_i \langle u_i \theta \rangle + \varepsilon) \right] \quad (1)$$

$$\begin{aligned} \langle u_i u_j \rangle = & \frac{\delta_{ij}}{3} q^2 - 3 \frac{l_1}{q} \left[\left(\langle u_k u_i \rangle - C_1 q^2 \delta_{ki} \right) \frac{\partial U_j}{\partial x_k} + \left(\langle u_k u_j \rangle - C_1 q^2 \delta_{kj} \right) \frac{\partial U_i}{\partial x_k} - \frac{2}{3} \delta_{ij} \langle u_k u_n \rangle \frac{\partial U_n}{\partial x_k} \right] \\ & - 3 \frac{l_1}{q} \beta \left[g_j \langle u_i \theta \rangle + g_i \langle u_j \theta \rangle - \frac{2}{3} \delta_{ij} g_n \langle u_n \theta \rangle \right] \end{aligned} \quad (2)$$

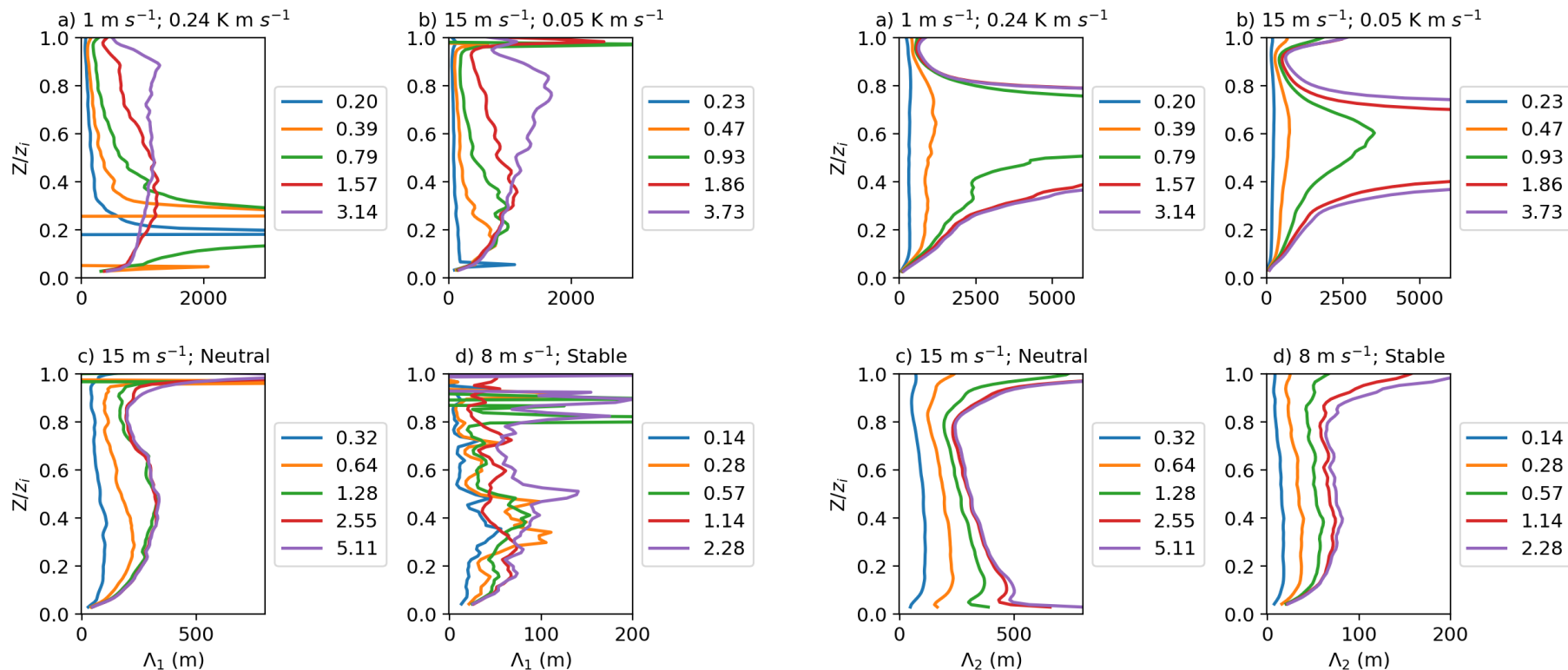
Eghdami et al. (2024), manuscript in preparation

$$\langle \theta^2 \rangle = - \frac{\Lambda_2}{q} \langle u_k \theta \rangle \frac{\partial \Theta}{\partial x_k} \quad (3)$$

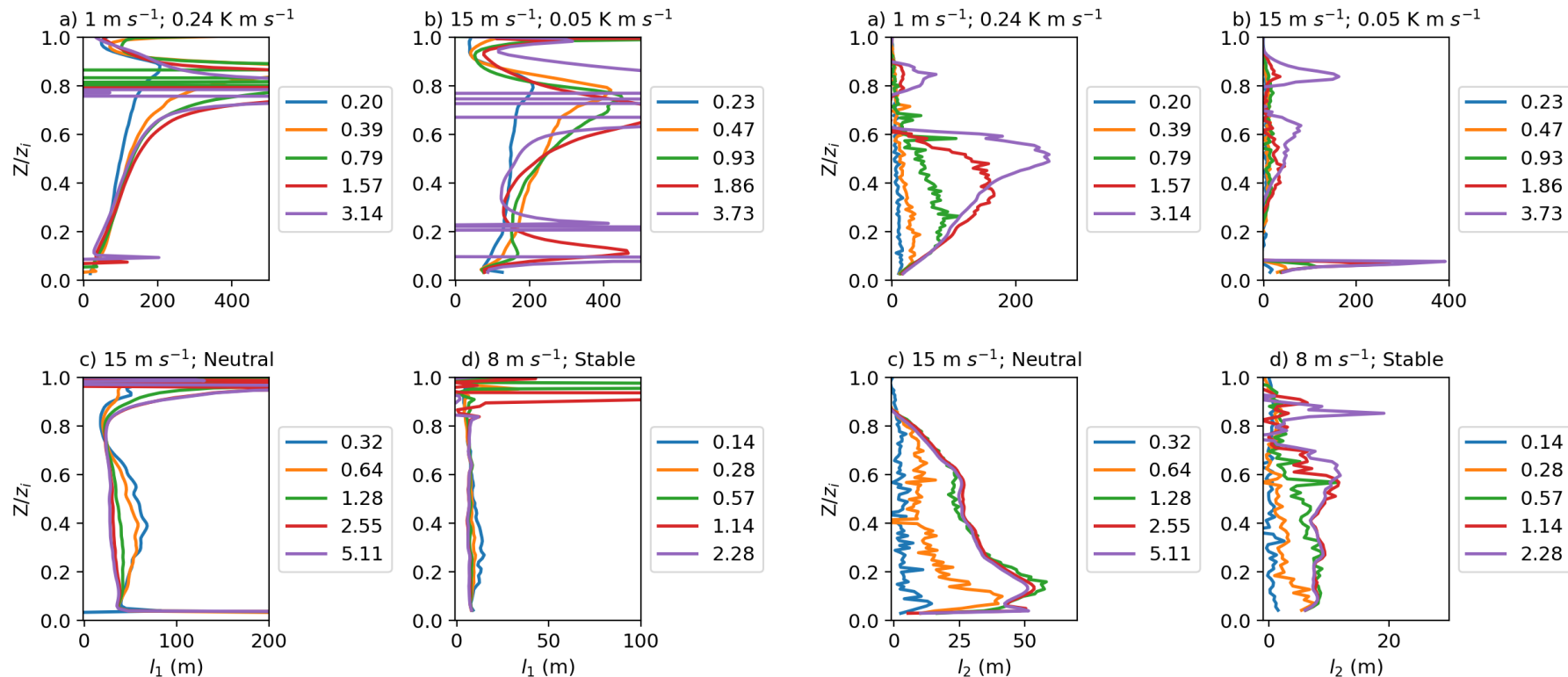
$$\langle u_j \theta \rangle = - 3 \frac{l_2}{q} \left[\langle u_j u_k \rangle \frac{\partial \Theta}{\partial x_k} + \langle u_k \theta \rangle \frac{\partial U_j}{\partial x_k} + \beta g_j \langle \theta^2 \rangle \right] \quad (4)$$

$$\varepsilon \equiv q^3 / \Lambda_1$$

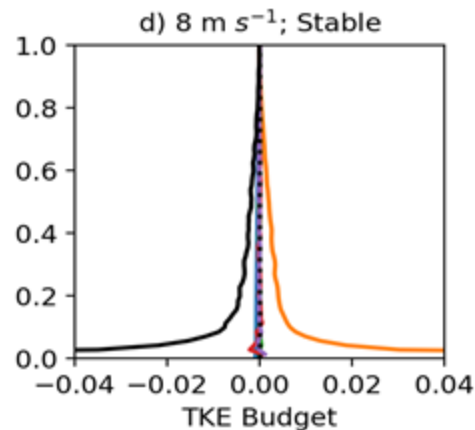
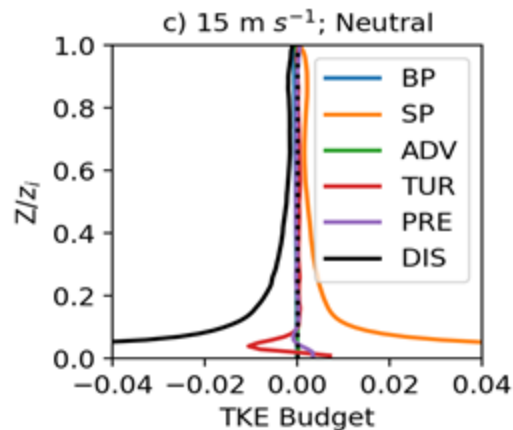
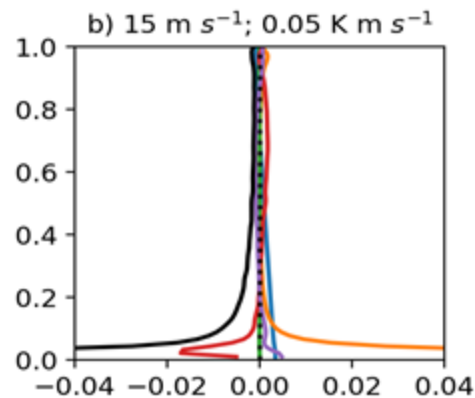
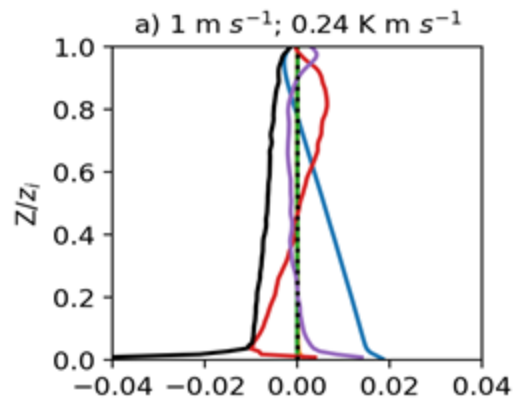
TKE and temperature variance dissipation length scales



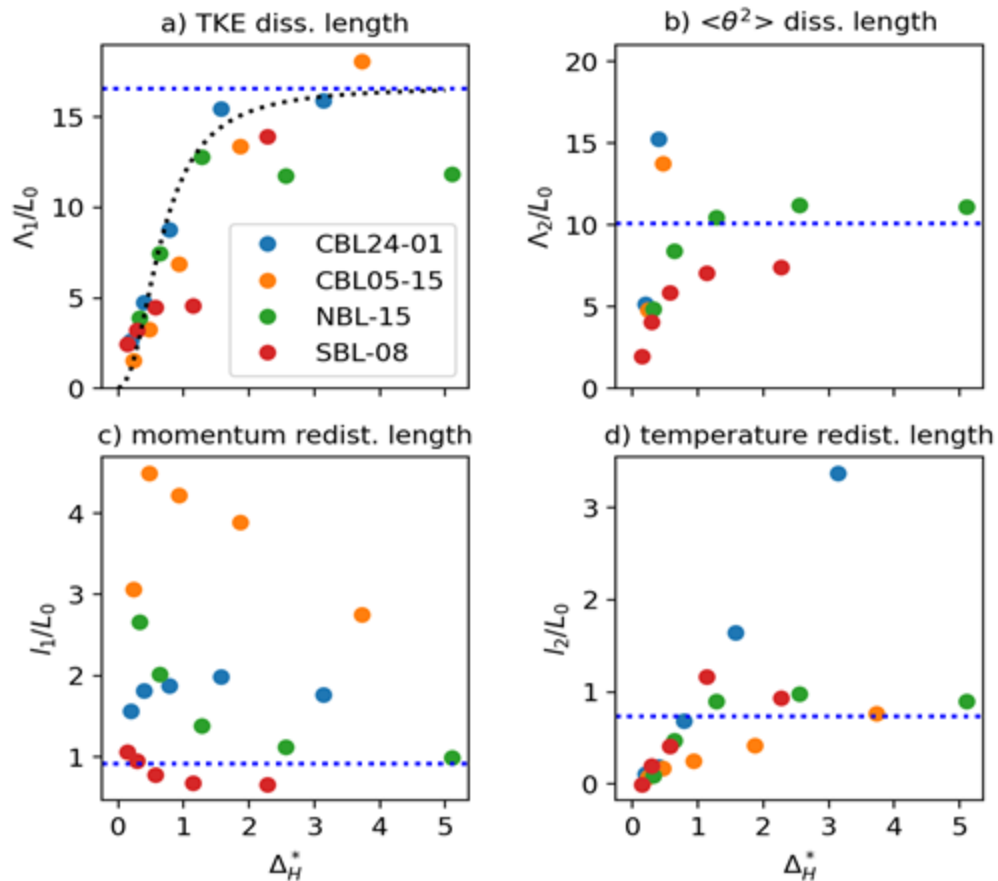
Pressure momentum and temperature redistribution length scales



TKE budgets for the four cases



Length scales as function of horizontal grid spacing



Some Final Thoughts

- Multiscale (meso- to micro-scale) simulations of atmospheric flows are needed for number of applications: wind energy, atmospheric dispersion, wildland fire prediction, urban air mobility, etc.
- Atmospheric flow predictions at microscale require coupling with mesoscale simulations
- Coupled, multiscale simulations required new developments:
 - Turbulence development at microscale
 - PBL parameterization in gray zone (100 m to 2 km)
 - Treatment of surface boundary condition
 - Enabling ensemble prediction to quantify uncertainty
- Developing PBL parameterization for the gray zone required abandoning the assumption of horizontal homogeneity over a grid cell
- Atmospheric flow modeling has reached the point where real-time large-eddy resolving simulations are possible, leading to prediction at microscale

Questions

branko.kosovic@jhu.edu

